FEBS Letters 494 (2001) 6–10 FEBS 24735

Hypothesis

A putative proton binding site of plasma membrane H^+-ATPase identified through homology modelling

Jens T. Bukrinsky[a,b], Morten J. Buch-Pedersen[b], Sine Larsen[a], Michael G. Palmgren[b,*]

[a] *Centre for Crystallographic Studies, Department of Chemistry, University of Copenhagen, Universitetsparken 5, DK-2100 Copenhagen, Denmark*
[b] *Department of Plant Biology, The Royal Veterinary and Agricultural University, Thorvaldsensvej 40, DK-1871 Frederiksberg C, Denmark*

Received 7 December 2000; revised 21 February 2001; accepted 8 March 2001

First published online 20 March 2001

Edited by Matti Saraste

Abstract We have used the 2.6 Å structure of the rabbit sarcoplasmic reticulum Ca^{2+}-ATPase isoform 1a, SERCA1a [Toyoshima, C., Nakasako, M., Nomura, H. and Ogawa, H. (2000) Nature 405, 647–655], to build models by homology modelling of two plasma membrane (PM) H^+-ATPases, *Arabidopsis thaliana* AHA2 and *Saccharomyces cerevisiae* PMA1. We propose that in both yeast and plant PM H^+-ATPases a strictly conserved aspartate in transmembrane segment (M)6 ($D684_{AHA2}$/$D730_{PMA1}$), and three backbone carbonyls in M4 ($I282_{AHA2}$/$I331_{PMA1}$, $G283_{AHA2}$/$I332_{PMA1}$ and $I285_{AHA2}$/$V334_{PMA1}$) comprise a binding site for H_3O^+, suggesting a previously unknown mechanism for transport of protons. Comparison with the structure of the SERCA1a made it feasible to suggest a possible receptor region for the C-terminal auto-inhibitory domain extending from the phosphorylation and anchor domains into the transmembrane region.

Key words: Auto-inhibition; H^+-ATPase; Hydronium ion; Proton binding site; Regulatory domain; Rabbit sarcoplasmic reticulum Ca^{2+}-ATPase isoform 1; Proton pump

1. Introduction

Plasma membrane (PM) H^+-ATPases are responsible for the ATP-fueled ejection of protons out of plant and yeast cells [1,2]. An electrochemical gradient of protons across the PM is hereby generated comprising the driving force for solute uptake through other PM transport systems. PM H^+-ATPases belong structurally and enzymatically to a large group of proteins termed P-type ATPases, also including the mammalian Na^+/K^+-, H^+/K^+-, PM Ca^{2+}-, and sarcoplasmic reticulum (SR) Ca^{2+}-ATPases. A characteristic feature of P-type ATPases is that a strictly conserved aspartate residue is phosphorylated during the reaction cycle (reviewed in [3]).

P-type ATPases consist of a single catalytic subunit and appear to have a very similar fold. Crystallographic images to 8 Å resolution from the *Neurospora* fungal PM H^+-ATPase reveal the presence of 10 transmembrane spanning helices (M1–M10) connected by a large cytoplasmic portion of the enzyme, and very little protein extending to the extracellular site of the cell [4]. In a comparison between this H^+ pump structure and an 8 Å resolution structure of the SERCA1a SR Ca^{2+}-ATPase [5] it was concluded that these pumps share a great deal of structural similarity especially pronounced in the membrane region, despite a relatively low level of amino acid homology [6]. The X-ray crystal structure of the SERCA1a Ca^{2+}-ATPase was recently determined to 2.6 Å resolution [7] and this structure has contributed with valuable knowledge and critical insights into the structure and mechanism of P-type ATPases. The cytoplasmic part of the protein is divided into three distinct parts: the nucleotide binding domain (N-domain), the phosphorylation domain (P-domain), and the actuator or anchor domain (A-domain) (Fig. 1). Many P-type ATPases, including PM H^+-ATPases, in addition contain terminal auto-inhibitory regulatory domains (R-domains) at either the extreme N- or C-terminus. The structural basis for auto-inhibition of these pumps is unknown.

Here we report a model for a putative proton binding site in the transmembrane region of two PM H^+-ATPases, AHA2 from *Arabidopsis thaliana* and PMA1 from *Saccharomyces cerevisiae*. The two models are produced by homology modelling based on the 2.6 Å resolution structure of SERCA1a.

2. Building the models of AHA2 and PMA1

The models were constructed using the coordinates from the structure of SERCA1a (Protein Data Base entry 1eul; [7]) with the programs Swiss-model and Swiss-pdb viewer [8,9]. Turbo-Frodo [10] was used as a graphical display program to visually validate the models and to adjust side chain conformations.

The major differences between the structure of SERCA1a (Fig. 1A) and the models of PMA1 (Fig. 1B) and AHA2 (Fig. 1C) are found in the N-domain, where large deletions in the sequences of PM H^+-ATPases had to be accounted for. The final model of PMA1 comprises residues 15–400, 408–484, 489–516 and 521–918, while that of AHA2 comprises the res-

*Corresponding author. Fax: (45)-3528-3365.
E-mail: palmgren@biobase.dk

Abbreviations: A-domain, actuator or anchor domain; ACA2, *Arabidopsis thaliana* auto-inhibited Ca^{2+}-ATPase isoform 2; AHA2, *Arabidopsis thaliana* PM H^+-ATPase isoform 2; M1–M10, transmembrane segments 1–10; N-domain, nucleotide binding domain; P-domain, phosphorylation domain; PM, plasma membrane; PMA1, *Saccharomyces cerevisiae* PM H^+-ATPase isoform 1; PMA2, *Nicotiana plumbaginifolia* PM H^+-ATPase isoform 2; R-domain, C-terminal regulatory domain; SERCA1a, rabbit SR Ca^{2+}-ATPase isoform 1a; SR, sarcoplasmic reticulum

PII: S0014-5793(01)02301-8

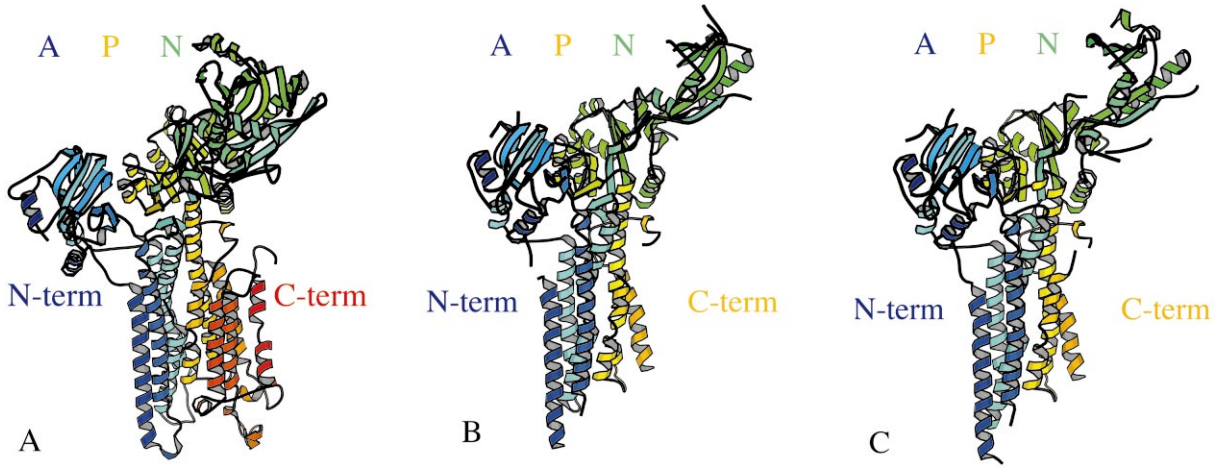

Fig. 1. Ribbon images of the X-ray structure of SERCA1a (A) and the most reliable part of the homology models of the PM H^+-ATPases AHA2 (B) and PMA1 (C). The structure of SERCA1a is according to Toyoshima et al. [7]. Ribbons are colored blue (N-terminus) through cyan, green, yellow, and orange to red (C-terminus). A, P and N denote A-, P- and N-domains, respectively. The figure was drawn using Molscript [26].

idues 1–21, 31–87, 92–191, 195–347, 358–382, 389–400, 406–467, 474–691, 698–812 and 820–912. For the gaps in the model the remaining residues would allow the chains to be ligated without geometric strain. The C-terminal hydrophilic portion of AHA2 and PMA1 was not included due to lack of this domain in the SR Ca^{2+}-ATPases. The last four transmembrane helices display very low sequence homology between the Ca^{2+}- and H^+-ATPases and different prediction models lead to slightly contradictory results in the assignment of secondary structure. We have therefore not included this part in our presentation of the models (Fig. 1B,C). All shown side chains are modelled in their most common rotamer. The essential parts of the models with highly conserved patches such as the phosphorylation site and the nucleotide binding site appeared to be fully superimposable on the structure of SERCA1a Ca^{2+}-ATPase (data not shown), indicating a good overall agreement of the structures modelled.

3. Proton transport

3.1. How does the PM H^+-ATPase transport protons across the cell membrane?

The mechanism of proton pumping by PM H^+-ATPases is not known. It has been suggested that PM H^+-ATPases pump protons via a proton-wire mechanism (reviewed in [11]). However, in other P-type ATPases cations appear to be translocated by a mechanism involving specific binding site(s) in the membrane, with the accessibility alternating between the two sites of the membrane during the catalytic cycle. Due to the biochemical and structural similarity to other P-type ATPases, a similar transport mechanism seems likely for the PM H^+-ATPase [12]. Transport of protons via a mechanism involving alternating access to a specific proton binding site(s) would probably require the transported species to be H_3O^+ rather than H^+ [11,13]. Specific binding of a transported H_3O^+ is likely to involve three or four liganding groups per bound H_3O^+ as hydrogen-bonding partners.

3.2. The region in H^+-ATPases corresponding to site I of SERCA1a

In the 2.6 Å structure of the SR Ca^{2+} pump, two Ca^{2+} ions are found in the transmembrane region [7] as seen in Fig. 2A. Site I (Fig. 2A, Ca^{2+} binding site located to the left) is located between M5 and M6, whereas site II (Fig. 2A, Ca^{2+} binding site located to the right) is located between M4 and M6. In site I, Ca^{2+} is interacting with three negatively charged residues $E771_{SERCA1a}$ (M5), $D800_{SERCA1a}$ (M6) and $E908_{SERCA1a}$ (M8). From sequence comparison of the transmembrane region of PM H^+-ATPases, it appears that only one negatively charged residue ($D684_{AHA2}$/$D730_{PMA1}$, corresponding to $D800_{SERCA1a}$; M6) is strictly conserved. The sequence comparisons also suggest that the negatively charged residues $E771_{SERCA1a}$ and $E908_{SERCA1a}$ could be replaced by $R655_{AHA2}$/$H701_{PMA1}$ (M5) and $Q795_{AHA2}$/$T837_{PMA1}$ (M8) with the latter localized in a more dubious part of the models.

In the model of AHA2, the guanidinium group of $R655_{AHA2}$ occupies a position equivalent to that occupied by Ca^{2+} in site I of SERCA1a. The side chain of $H701_{PMA1}$ also protrudes into this region. Thus, according to our models, binding of H_3O^+ seems very unlikely at this location in both PM H^+-ATPases. An arginine ($R695_{PMA1}$) located six residues upstream from $H701_{PMA1}$ is conserved in the fungal PM H^+-ATPases (see the P-type ATPase database http://www.biobase.dk/~axe/Patbase.html). Based on genetic studies it was suggested that $R695_{PMA1}$ is linked by a salt bridge to $D730_{PMA1}$ in M6 [14]. The formation of this salt bridge is not confirmed by the homology model of PMA1, as it would require dramatic changes of modelled structure. It should be noted that significant distortions of the model are also necessary when an alternative sequence alignment of M5 [14] was used.

3.3. The region in H^+-ATPases corresponding to site II of SERCA1a

Ca^{2+} binding site II of SERCA1a is formed by side chain oxygen atoms of $E309_{SERCA1a}$ (M4), $N796_{SERCA1a}$ (M6) and $D800_{SERCA1a}$ (M6) and three carbonyl oxygen atoms from M4 (those of $V304_{SERCA1a}$, $A305_{SERCA1a}$ and $I307_{SERCA1a}$) (Fig. 2A). In a perfect α-helix all backbone carbonyl groups are involved in hydrogen-bonding with the backbone amide from the residue positioned +4 relative to the first. The carbonyl groups are exposed only if the helix is perturbed from

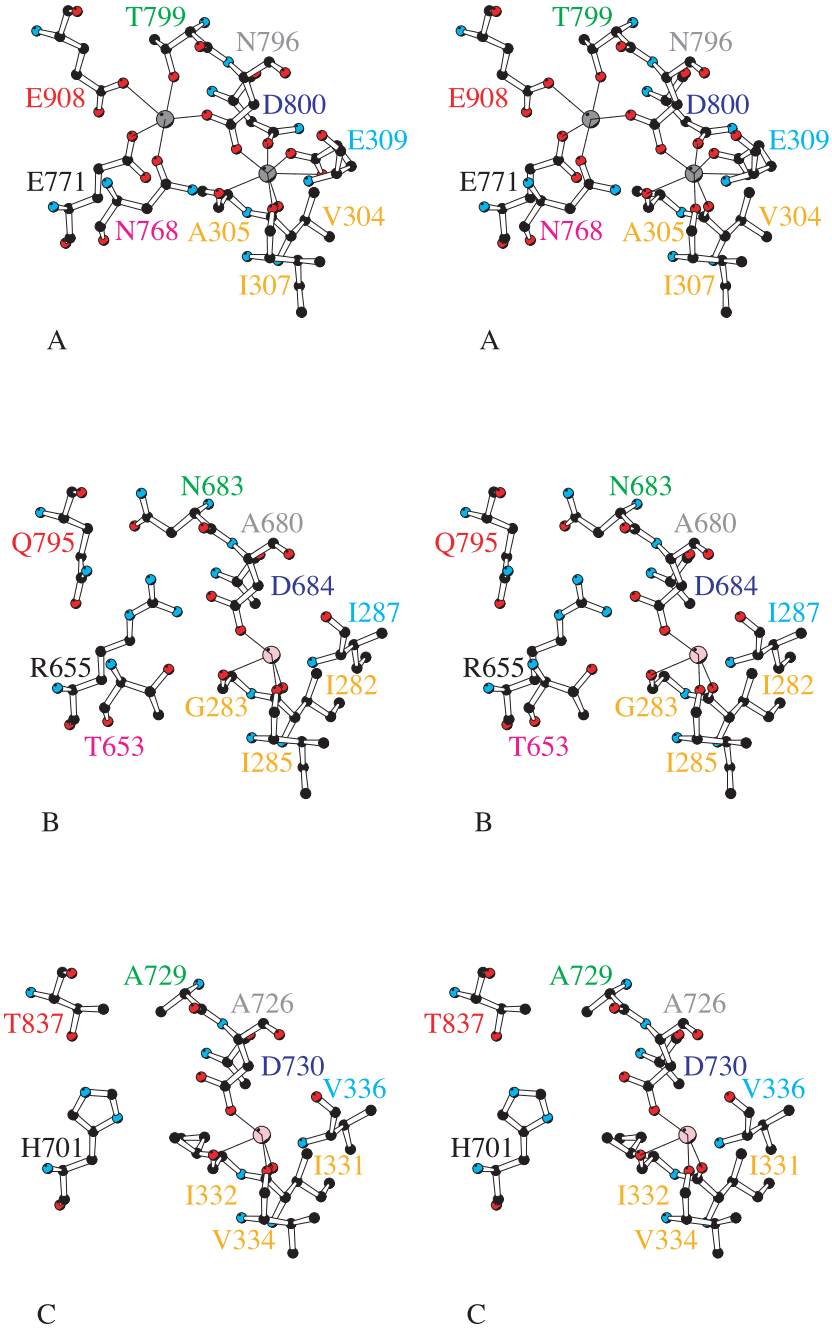

Fig. 2. Stereo view of the Ca^{2+} binding site of SERCA1a (A) and the proposed H_3O^+ binding sites in the PM H^+-ATPases AHA2 (B) and PMA1 (C). All sites are shown with the same orientation. In the structure of SERCA1a [7], the Ca^{2+} ions are shown as gray spheres. The Ca^{2+} ions to the left and right are bound to site I and site II, respectively. In the PM H^+-ATPase models, a putative H_3O^+ in site II is shown as a pink sphere. Residues with identical label colors are structurally aligned in the models. The figure was drawn using Molscript [26]. $Q795_{AHA2}/T837_{PMA1}$ are positioned in a less reliable part of the model.

ideal bonding geometry. Two proline residues, $P308_{SERCA1a}$ and $P312_{SERCA1a}$, introduce unwinding of M4 by twisting of the backbone, in this way depriving the carbonyls of their natural hydrogen-bonding partners. The PM H^+-ATPases contain proline residues in equivalent positions which are strictly conserved ($P286_{AHA2}/P335_{PMA1}$ and $P290_{AHA2}/P339_{PMA1}$) suggesting that M4 is also unwound in these pumps. In the homology models of AHA2 and PMA1, the backbone carbonyls of $I282_{AHA2}/I331_{PMA1}$, $G283_{AHA2}/I332_{PMA1}$ and $I285_{AHA2}/V334_{PMA1}$, respectively, could contribute to a hydronium ion binding site.

3.4. The proposed H^+ binding site

The two homology models predict that one potential hydronium ion binding site is likely to be positioned in the region corresponding to Ca^{2+} binding site II. Three backbone carbonyls (those of $I282_{AHA2}/I331_{PMA1}$, $G283_{AHA2}/I332_{PMA1}$ and $I285_{AHA2}/V334_{PMA1}$) comprise the hydrogen-bonding partners to H_3O^+ and the carboxylic group of $D684_{AHA2}/D730_{PMA1}$ could be sharing a proton with a bound hydronium ion and/or with $R655_{AHA2}/H701_{PMA1}$.

Experimental evidence points to a role for $D684_{AHA2}$ in the transport mechanism of AHA2. Thus, a $D684N_{AHA2}$ substi-

tution results in total abolishment of proton pumping [15]. The mutated enzyme is able to hydrolyze ATP but is blocked during its catalytic cycle immediately following formation of the E_1P phospho-intermediate. This suggests that the negatively charged side chain of $D684_{AHA2}$ interacts with the transported species and is essential for proton translocation although it may not be essential for binding to occur [15]. Efforts to express corresponding $D730_{PMA1}$ mutants were unsuccessful [14].

In SERCA1a five negatively charged residues, two polar residues and three backbone carbonyls form the binding sites for two Ca^{2+} ions. However, in PM H^+-ATPases only one negatively charged residue is strictly conserved ($D684_{AHA2}$/$D730_{PMA1}$). The region corresponding to Ca^{2+} binding site I in the homology models is unlikely to be able to bind H_3O^+ due to the lack of excess negative charge. Furthermore, $R655_{AHA2}$/$H701_{PMA1}$ is protruding into the region where Ca^{2+} is bound in SERCA1a. Excess of negative charge is found only in the region corresponding to Ca^{2+} site II and originates from the aspartate ($D684_{AHA2}$/$D730_{PMA1}$), the backbone carbonyls, and the helix dipole. In this otherwise hydrophobic environment a bound water molecule would tend to become protonated. This region in PM H^+-ATPases would thus have a relatively high affinity for one hydronium ion.

4. Regulation and auto-inhibition of PM H^+-ATPases

4.1. *In vivo and in vitro regulation of PM H^+-ATPases*

The activities of plant and yeast PM H^+-ATPases are down-regulated by an inhibitory domain located in the extreme C-terminus of the enzyme (R-domain). Deletion of the R-domain, either at the gene level [16,17] or by trypsin treatment [18,19], results in constitutively activated H^+-ATPases. The R-domain is likely to interact with a specific intramolecular receptor of the pump and in this way to exert its negative effect on enzyme activity. Based on peptide cross-linking studies, it has been proposed that the C-terminal R-domain of human PM Ca^{2+}-ATPase hPMCA4 interacts with the A-domain [20] and the N-domain [21] of this pump.

Using genetic approaches, a large number of amino acid residue substitutions leading to increased pump activity of *S. cerevisiae* (PMA1) [22] and *Nicotiana plumbaginifolia* (PMA2) [23,24] PM H^+-ATPases have been identified. These mutations, apart from those in the R-domain, are localized in the A-, N- and P-domains as well as in transmembrane regions. A similar strategy was used to identify regulatory mutants in *A. thaliana* (ACA2), a Ca^{2+} pump regulated by an N-terminal auto-inhibitory domain [25]. Such genetic information can be interpreted as evidence for domain interactions.

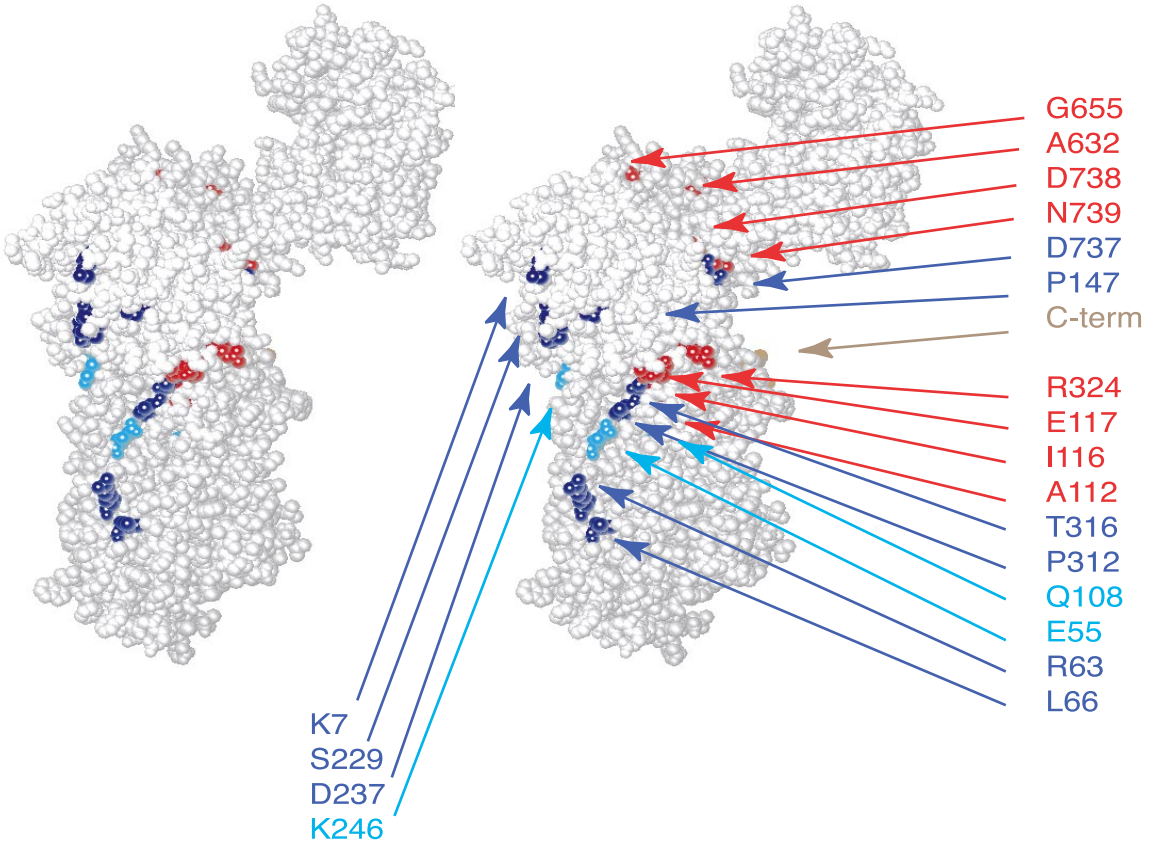

Fig. 3. Space-filling image in stereo view of the SERCA1a structure. Corresponding residues in *S. cerevisiae* PM H^+-ATPase PMA1 [22], *N. plumbaginifolia* PM H^+-ATPase PMA2 [23,24] and the *A. thaliana* endoplasmic reticulum Ca^{2+}-ATPase ACA2 [25] that give rise to activated mutants when substituted are indicated in red, blue, and green, respectively. The C-terminal is indicated in brown. Protein sequences were aligned using the Clustal W Multiple Sequence Alignment Program [27]. The indicated PMA1 residues correspond to the following SERCA1a residues: $A165_{PMA1}$/$A112_{SERCA1}$, ($V169–D170_{PMA1}$)/($I116–E117)_{SERCA1}$, $A351_{PMA1}$/$R324_{SERCA1}$, $A565_{PMA1}$/$A632_{SERCA1}$, $G587_{PMA1}$/$G655_{SERCA1}$, $P669_{PMA1}$/$D738_{SERCA1}$, and $G670_{PMA1}$/$N739_{SERCA1}$. Residues in PMA2 correspond to residues in SERCA1a as follows: $E14_{PMA2}$/$K7_{SERCA1}$, $P72_{PMA2}$/$R63_{SERCA1}$, $W75_{PMA2}$/$L66_{SERCA1}$, $P154_{PMA2}$/$P147_{SERCA1}$, $H221_{PMA2}$/$S229_{SERCA1}$, $H229_{PMA2}$/$D237_{SERCA1}$, $P294_{PMA2}$/$P312_{SERCA1}$, $S298_{PMA2}$/$T316_{SERCA1}$ and $E626_{PMA2}$/$D737_{SERCA1}$. Residues in ACA2 correspond to the following SERCA1a residues: $E167_{ACA2}$/$E55_{SERCA1}$, $D219_{ACA2}$/$Q108_{SERCA1a}$ and $E341_{ACA2}$/$K246_{SERCA1}$. The figure was made with Turbo-Frodo [10].

However, because the mutations are scattered throughout the primary structure of the pumps, it has been difficult to build a model for the R-domain interactions.

4.2. Structural basis of the regulation of PM H^+-ATPases

The residues in SERCA1a that correspond to the residues in *S. cerevisiae* PMA1, *N. plumbaginifolia* PMA2, and *A. thaliana* ACA2 that lead to an activated enzyme when substituted are indicated in the space-filling image of SERCA1a shown in Fig. 3. Most of these residues cluster on the surface of the pump where they form an almost continuous line extending from the P-domain to the middle of M1 (Fig. 3). A similar pattern is revealed if the mutants are marked in the modelled structures of AHA2 and PMA1 (data not shown). This suggests that the C-terminus in the non-activated pump docks onto the ATPase molecule in a path running from the P-domain to the middle of the membrane in a plane almost perpendicular to the membrane. The C-terminal domain of plant PM H^+-ATPases is approximately 60 residues longer than that of fungal H^+-ATPases [19] and may therefore be able to extend further into the membrane than its yeast counterpart.

Acknowledgements: We thank Thomas H. Roberts for helpful comments on the manuscript. Henning Osholm Sørensen is acknowledged for his assistance with the figure production. This work was supported by the Human Frontier Science Program Organization, the European Unions Biotechnology Program, by a fellowship from the Danish International Developmental Agency (M.B.P.).

References

[1] Morsomme, P., Slayman, C.W. and Goffeau, A. (2000) Biochim. Biophys. Acta 1469, 133–157.
[2] Palmgren, M.G. (2001) Annu. Rev. Plant Physiol. Plant Mol. Biol. 53, 817–845.
[3] Møller, J.V., Juul, B. and Le Maire, M. (1996) Biochim. Biophys. Acta 1286, 1–51.
[4] Auer, M., Scarborough, G.A. and Kühlbrandt, W. (1998) Nature 392, 840–843.
[5] Zhang, P., Toyoshima, C., Yonekura, K., Green, N.M. and Stokes, D.L. (1998) Nature 392, 835–839.
[6] Kühlbrandt, W., Auer, M. and Scarborough, G.A. (1998) Curr. Opin. Struct. Biol. 8, 510–516.
[7] Toyoshima, C., Nakasako, M., Nomura, H. and Ogawa, H. (2000) Nature 405, 647–655.
[8] Guex, N. and Peitsch, M.C. (1997) Electrophoresis 18, 2714–2723.
[9] Peitsch, M.C. (1996) Biochem. Soc. Trans. 24, 274–279.
[10] Roussel, A. and Cambillau, C. (1992) TURBO-FRODO, Biographics and AFMB (Architecture et Function des Macromolecules Biologiques), Marseille.
[11] Briskin, D.P. and Hanson, J.B. (1992) J. Exp. Bot. 43, 269–289.
[12] Serrano, R. (1989) Annu. Rev. Plant Physiol. Plant Mol. Biol. 40, 61–94.
[13] Boyer, P.D. (1988) Trends Biochem. Sci. 13, 5–7.
[14] Gupta, S.S., DeWitt, N.D., Allen, K.E. and Slayman, C.W. (1998) J. Biol. Chem. 273, 34328–34334.
[15] Buch-Pedersen, M.J., Venema, K., Serrano, R. and Palmgren, M.G. (2000) J. Biol. Chem. 275, 39167–39173.
[16] Portillo, F., de Larrinoa, I.F. and Serrano, R. (1989) FEBS Lett. 247, 381–385.
[17] Palmgren, M.G. and Christensen, G. (1993) FEBS Lett. 317, 216–222.
[18] Palmgren, M.G., Larsson, C. and Sommarin, M. (1990) J. Biol. Chem. 265, 13423–13426.
[19] Palmgren, M.G., Sommarin, M., Serrano, R. and Larsson, C. (1991) J. Biol. Chem. 266, 20470–20475.
[20] Falchetto, R., Vorherr, T., Brunner, J. and Carafoli, E. (1991) J. Biol. Chem. 266, 2930–2936.
[21] Falchetto, R., Vorherr, T. and Carafoli, E. (1992) Protein Sci. 1, 1613–1621.
[22] Eraso, P. and Portillo, F. (1994) J. Biol. Chem. 269, 10393–10399.
[23] Morsomme, P., de Kerchove d'Exaerde, A., De Meester, S., Thines, D., Goffeau, A. and Boutry, M. (1996) EMBO J. 15, 5513–5526.
[24] Morsomme, P., Dambly, S., Maudoux, O. and Boutry, M. (1998) J. Biol. Chem. 273, 34837–34842.
[25] Curran, A.C., Hwang, I., Corbin, J., Martinez, S., Rayle, D., Sze, H. and Harper, J.F. (2000) J. Biol. Chem. 275, 30301–30308.
[26] Krulis, P.J. (1991) J. Appl. Crystallogr. 24, 946–950.
[27] Thompson, J.D., Higgins, D.G. and Gibson, T.J. (1994) Nucleic Acids Res. 22, 4673–4680.